Anti-inflammatory spiroditerpenoids from *Penicillium bialowiezense*

Jaeyoung Kwon [a],[1], Min Jee Kim [b],[1], Dong-Cheol Kim [c], Haeun Kwon [b], Seung Mok Ryu [d],
Sang Hee Shim [e], Yuanqiang Guo [f], Seung-Beom Hong [g], Joung Han Yim [h], Youn-Chul Kim [c],
Hyuncheol Oh [c], Dongho Lee [b],[*]

[a] *Natural Product Informatics Research Center, Korea Institute of Science and Technology (KIST) Gangneung Institute, Gangneung 25451, Republic of Korea*
[b] *Department of Plant Biotechnology, College of Life Sciences and Biotechnology, Korea University, Seoul 02841, Republic of Korea*
[c] *Institute of Pharmaceutical Research and Development, College of Pharmacy, Wonkwang University, Iksan 54538, Republic of Korea*
[d] *Herbal Medicine Resources Research Center, Korea Institute of Oriental Medicine, Naju 58245, Republic of Korea*
[e] *Natural Products Research Institute, College of Pharmacy, Seoul National University, Seoul 08826, Republic of Korea*
[f] *State Key Laboratory of Medicinal Chemical Biology, College of Pharmacy, and Tianjin Key Laboratory of Molecular Drug Research, Nankai University, Tianjin 300071, People's Republic of China*
[g] *Korean Agricultural Culture Collection, National Institute of Agricultural Science, Wanju 55365, Republic of Korea*
[h] *Korea Polar Research Institute, Korea Ocean Research and Development Institute, Incheon 21990, Republic of Korea*

ARTICLE INFO

ABSTRACT

Inflammation is a vital process that maintains tissue homeostasis. However, it is widely known that uncontrolled inflammation can contribute to the development of various diseases. This study aimed to discover anti-inflammatory metabolites from *Penicillium bialowiezense*. Seven spiroditerpenoids, including two new compounds, breviones P and Q (**1** and **2**), were isolated and characterized by various spectroscopic and spectrometric methods. All isolated compounds were initially tested for their inhibitory effects against lipopolysaccharide-induced nitric oxide (NO) production in RAW 264.7 macrophages. Of these, brevione A (**3**) exhibited this activity with a half-maximal inhibitory concentration value of 9.5 μM. Further mechanistic studies demonstrated that **3** could suppress the expression of pro-inflammatory cytokines and mediators, such as NO, prostaglandin E_2, interleukin (IL)-1β, tumor necrosis factor-α, IL-6, and IL-12 by inhibiting the activation of nuclear factor-kappa B and c-Jun *N*-terminal kinase.

1. Introduction

Inflammation is a protective response to harmful stimuli, including pathogen invasion. It is a critical procedure that the body can utilize to signal the immune system to maintain tissue homeostasis [1]. However, failure to control inflammation can cause pathological changes that contribute to acute or chronic diseases. Many diseases, such as Alzheimer's disease, arthritis, and cancer, are associated with inflammation [1]. For this reason, controlling inflammation using various classes of molecules has been considered a prospective strategy to treat or prevent diseases. Although a lot of lead compounds have been proposed and some of them including nonsteroidal anti-inflammatory drugs, gluco-corticoids, and immunosuppressant drugs have been approved, therapy using these drugs is often still hampered due to insufficient effects or adverse effects such as gastrointestinal or renal side effects. Thus,

discovering new and potent inhibitors of inflammation is still in great demand in academia and industry [2]. Natural products, especially microbes and plants, have played a critical role in discovering these molecules, as they contain a rich suite of secondary metabolites [3–5]. Various studies have shown that natural product-derived compounds can control inflammatory responses and mediate signaling pathways, such as nuclear factor-kappa B (NF-κB) and mitogen-activated protein kinases (MAPKs) [6,7].

Meroterpenoids are naturally occurring compounds of mixed biosynthetic origin. These compounds, which are commonly isolated from fungi, display diverse chemical structures with a range of biological activities, including antimicrobial, anticancer, anti-inflammatory, and immunosuppressive effects [8]. In particular, breviones are an important group that contains a breviane spiroditerpenoid framework produced by the hybrid polyketide and terpenoid pathways [8]. These
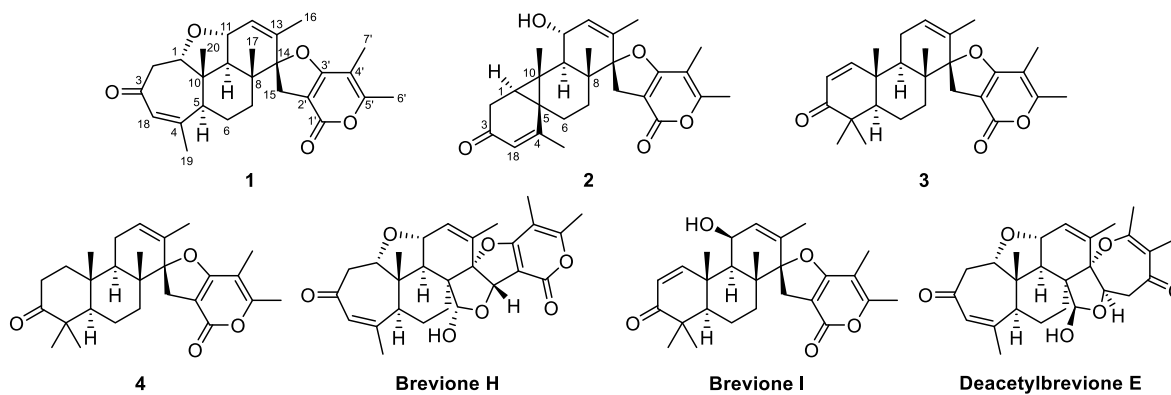
Fig. 1. Structures of all isolated compounds.

biosynthetic pathways confer structural complexity and diversity with biological activities. Since brevione A was first isolated from *Penicillium* sp. [9], a total of 15 naturally occurring compounds exhibiting allelopathic, anti-human immunodeficiency virus, anti-cancer, and anti-beta-amyloid effects have been reported [9–13].

In our ongoing research on anti-inflammatory compounds from fungi [6,14], we isolated seven breviones from *Penicillium bialowiezense* (Fig. 1). Compounds **1** and **2** were characterized as new structures by spectroscopic and spectrometric techniques. All isolated compounds were initially screened for their inhibitory effects of nitric oxide (NO) production in lipopolysaccharide (LPS)-activated RAW264.7 cells, which led to further mechanistic studies using brevione A (**3**). This paper reports the isolation, structural elucidation, and anti-inflammatory evaluation of the isolated compounds.

2. Experimental

2.1. General experimental procedures

Optical rotation, ultraviolet (UV), infrared (IR), and electronic circular dichroism (ECD) data were obtained using a Jasco P-2000 digital polarimeter (Tokyo, Japan), an Optizen spectrophotometer (Daejeon, Republic of Korea), an Agilent Cary 630 FTIR spectrometer (Santa Clara, CA, USA), and a Jasco J-1100 CD spectrometer, respectively. Nuclear magnetic resonance (NMR) spectra were recorded on a Varian 500 MHz NMR spectrometer (Palo Alto, CA, USA) in acetone-d_6 containing D_2O and tetramethylsilane. High-resolution electrospray ionization mass spectrometry (HRESIMS) data were collected on a Waters Q-TOF mass spectrometer (Milford, MA, USA). The medium pressure liquid chromatography (MPLC) system utilized a Biotage Isolera One (Uppsala, Sweden) with silica gel in SNAP cartridge (25 g, 72 × 30 mm i.d.). Preparative-high performance liquid chromatography (prep-HPLC) separation was performed on a Varian system with an YMC ODS-A column (5 μm, 250 × 20 mm i.d.) (Kyoto, Japan). Flash column chromatography was carried out using an YMC reverse-phased (RP)-C_{18} resin. Roswell Park Memorial Institute 1640 (RPMI 1640) medium, fetal bovine serum (FBS), and cell culture reagents were obtained from Gibco BRL (Grand Island, NY, USA). All other chemicals were obtained from Sigma-Aldrich (St. Louis, MO, USA) unless otherwise indicated. Antibodies were purchased from Santa Cruz Biotechnology (Santa Cruz, CA, USA). An enzyme-linked immunosorbent assay (ELISA) kit was obtained from R&D Systems (Minneapolis, MN, USA) Dimethylsulfoxide was used as a negative control of all biological evaluations.

2.2. Fungal material and fermentation

P. bialowiezense KACC 45970 was obtained from the Korean Agricultural and Culture Collection (KACC), Wanju, Republic of Korea. The strain was identified using the *β*-tubulin gene (S2, Supplementary

Table 1
NMR spectroscopic data for compounds **1** and **2** in acetone-d_6 with D_2O.

Position	1		2	
	δ_C	δ_H (*J* in Hz)	δ_C	δ_H (*J* in Hz)
1	86.3	3.77 dd (13.0, 3.0)	34.9	1.32 d (9.0)
2	49.3	2.96 dd (15.0, 13.0)	32.6	2.63 dd (20.0, 9.0)
		2.59 dd (15.0, 3.0)		2.42 dd (20.0, 1.0)
3	197.6		197.5	
4	163.0		164.3	
5	46.2	2.99 d (11.0)	27.6	
6	22.7	2.10 m	27.3	2.29 ddd (14.0, 5.0, 5.0)
		1.98 m		1.40 m
7	30.4	1.75 m	31.1	1.66 m
		1.58 m		1.49 m
8	41.2		41.4	
9	51.2	2.15 d (11.0)	50.6	1.89 d (10.5)
10	46.4		28.2	
11	74.4	4.27 ddd (11.5, 2.0, 2.0)	67.6	4.35 ddd (10.0, 2.5, 2.0)
12	127.9	5.95 br s	133.6	5.72 br s
13	137.7		132.4	
14	100.1		100.5	
15	29.3	3.10 d (16.0)	30.3	3.02 d (16.0)
		2.98 d (16.0)		2.93 d (16.0)
16	19.1	1.74 s	18.2	1.68 s
17	16.2	1.10 s	20.0	1.13 s
18	130.6	5.83 br d (1.0)	127.0	5.85 br d (1.0)
19	23.0	1.98 s	23.1	2.10 s
20	18.7	1.25 s	10.4	1.15 s
1′	171.2		172.0	
2′	100.3		100.2	
3′	161.9		161.9	
4′	103.5		103.4	
5′	161.8		161.8	
6′	9.5	1.96 s	9.5	1.91 s
7′	17.2	2.22 s	17.2	2.22 s

material) and detailed information is on the KACC website (http://genebank.rda.go.kr). Solid fermentation of the fungus was carried out on 75 Petri dishes (150 mm × 20 mm) with potato dextrose agar at 25 °C for 13 days.

2.3. Extraction and isolation of compounds

The fermented cultures were extracted with methanol (MeOH, 2 × 2 L). The solvent was concentrated until MeOH was completely removed; partitioning was then carried out using water (H_2O, 2 L) and ethyl acetate (EtOAc, 2 × 2 L) to acquire the EtOAc layer (1.2 g). The obtained layer was separated by MPLC using two SNAP cartridges connected (2 × 25 g) and eluted with chloroform–MeOH (2 × 25 g, $CHCl_3$–MeOH, 1:0 to 0:1 in 10 min, 50 mL/min) to yield 20 fractions (F1 to F20). F10 (84.4 mg) was purified by prep-HPLC (MeOH–H_2O, 1:1 to 7:3 in 60 min, 8 mL/min) to obtain brevione H (3.8 mg, t_R 25.6 min) and deacetylbrevione E

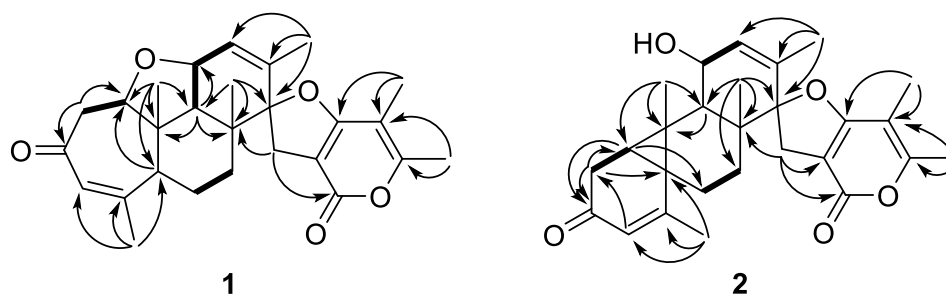**Fig. 2.** COSY and HMBC NMR correlations of compounds **1** and **2**.

(3.0 mg, t_R 33.2 min). F9 (279.1 mg) was separated on an RP-C$_{18}$ column (3.6 g, 180 × 10 mm i.d., MeOH–H$_2$O, 2:8 to 1:0) to obtain 11 fractions (F9-1 to F9-11). F9-6 (21.5 mg) was separated by prep-HPLC (MeOH–H$_2$O, 57:43 to 3:2 in 60 min, 8 mL/min) to obtain brevione P (**1**, 1.4 mg, t_R 26.1 min), and the residue was again purified by prep-HPLC (MeOH–H$_2$O, 1:1 to 3:2 in 60 min, 8 mL/min) to obtain brevione Q (**2**, 1.7 mg, t_R 32.5 min). F9-7 (34.3 mg) was separated by prep-HPLC (MeOH–H$_2$O, 3:2 to 7:3 in 60 min, 8 mL/min) to obtain brevione I (6.8 mg, t_R 28.9 min). F9-8 (12.0 mg) was purified by prep-HPLC (MeOH–H$_2$O, 6:4 to 1:0 in 60 min, 8 mL/min) to obtain brevione A (**3**, 6.0 mg, t_R 30.0 min). F9-9 (26.3 mg) was purified by prep-HPLC (MeOH–H$_2$O, 7:3 to 9:1 in 60 min, 8 mL/min) to obtain brevione B (**4**, 11.6 mg, t_R 27.8 min).

2.3.1. Brevione P (1)

White solid; $[\alpha]^{26}_D$ + 63.6 (*c* 0.02, MeOH); UV (MeOH) λ_{max} (log ε) 213 (3.80), 245 (3.55), 296 (3.15) nm; IR ν_{max} (ATR) 2923, 1718, 1648, 1436, 1201, 1115 cm^{-1}; ECD (c 0.13 mM, MeOH) $\Delta\varepsilon$ + 13.3 (217), 15.1 (241); ^{1}H and ^{13}C NMR (500 and 125 MHz, acetone-d_6 + D$_2$O), see Table 1; ESIMS (positive) *m/z* 437 [M + H]$^+$; HRESIMS (positive) *m/z* 437.2344 [M + H]$^+$ (calcd for C$_{27}$H$_{33}$O$_5$, 437.2328).

2.3.2. Brevione Q (2)

White solid; $[\alpha]^{26}_D$ + 34.4 (*c* 0.02, MeOH); UV (MeOH) λ_{max} (log ε) 212 (3.85), 284 (3.15) nm; IR ν_{max} (ATR) 2969, 1684, 1437, 1277, 1202, 1134, 1025 cm^{-1}; ECD (c 0.13 mM, MeOH) $\Delta\varepsilon$ + 8.8 (214), +2.3 (239), 3.1 (329); ^{1}H and ^{13}C NMR (500 and 125 MHz, acetone-d_6 + D$_2$O), see Table 1; ESIMS (positive) *m/z* 437 [M + H]$^+$; HRESIMS (positive) *m/z* 437.2336 [M + H]$^+$ (calcd for C$_{27}$H$_{33}$O$_5$, 437.2328).

2.4. Computational methods

Computational methods were conducted based on previous studies [15]. Briefly, conformational analysis was carried out using the molecular mechanics force field model of Spartan' 14 software (Wavefunction, Irvine, CA, USA). Geometry optimization and energy calculation were performed using density functional theory (DFT) and time-dependent DFT calculations, respectively, in Gaussian 09 software (Gaussian, Wallingford, CT, USA).

2.5. Cell culture and viable assay

RAW 264.7 cells were grown at 37 °C in an atmosphere containing 5% CO$_2$ in RPMI 1640 medium supplemented with 10% FBS, 100 U/mL penicillin G, 100 μg/mL streptomycin, and 2 mM L-glutamine. Viability was measured using an MTT assay as previously described [6].

2.6. Measurement of NO and PGE$_2$ production and cytokine assay

Cells in 24-well plates were pretreated with various concentrations of **3** for 3 h and then stimulated with LPS (1 μg/mL) for 24 h. For the measurement of NO production, the Griess reaction was used to monitor

nitrite levels as an indicator. To measure prostaglandin E$_2$ (PGE$_2$), interleukin (IL)-1β, tumor necrosis factor-α (TNF-α), IL-6, and IL-12 levels, an ELISA kit was used based on the manufacturer's recommendations. The assays were conducted as previously reported [6].

2.7. Quantitative real-time RT-PCR

Total RNA was obtained using a Trizol kit (Invitrogen, Carlsbad, CA, USA), quantified at 260 nm, and reverse transcribed with a High-Capacity RNA-to-cDNA kit (Applied Biosystems, Carlsbad, CA, USA). The cDNA was amplified using a SYBR Premix Ex Taq kit (Takara Bio, Shiga, Japan). Detailed procedures have been described previously [6].

2.8. Preparation of cytosolic and nuclear fractions

Cells were lysed using a Mammalian Protein Extraction Reagent kit (Pierce Biotechnology, Rockford, IL, USA) with protease inhibitor cocktail I (EMD Biosciences, San Diego, CA, USA) and 1 mM phenylmethylsulfonyl fluoride. The cytosolic fraction was obtained by centrifugation. Nuclear and cytoplasmic fractions were obtained using a Nuclear and Cytoplasmic Extraction Reagent kit (Pierce Biotechnology), respectively. Detailed procedures have been described previously [6].

2.9. DNA binding activity of NF-κB

Cells were pretreated with various concentrations of **3** for 3h and then treated with LPS for 1 h. The DNA-binding activity of NF-κB was measured using a TransAM kit (Active Motif, Carlsbad, CA, USA). Detailed procedures have been described previously [6].

2.10. Western blot analysis

Cells were harvested, pelleted, washed with phosphate-buffered saline, and lysed using 20 mM Tris-HCl buffer with a protease inhibitor mixture. The concentration was determined using a Lowry protein assay kit (Sigma-Aldrich). Detailed procedures have been described previously [6].

2.11. Statistical analysis

All experiments were conducted at least three times. All data are expressed as the mean ± standard deviation. One-way analysis of variance was carried out for multiple comparisons followed by Tukey's multiple comparison test.

3. Results and discussion

3.1. Structural characterization of compounds

Compound **1** was obtained as a white solid. The molecular formula was determined to be C$_{27}$H$_{32}$O$_5$ based on the HRESIMS data, showing 12 indices of hydrogen deficiency. The UV absorption at 213, 245, and 296
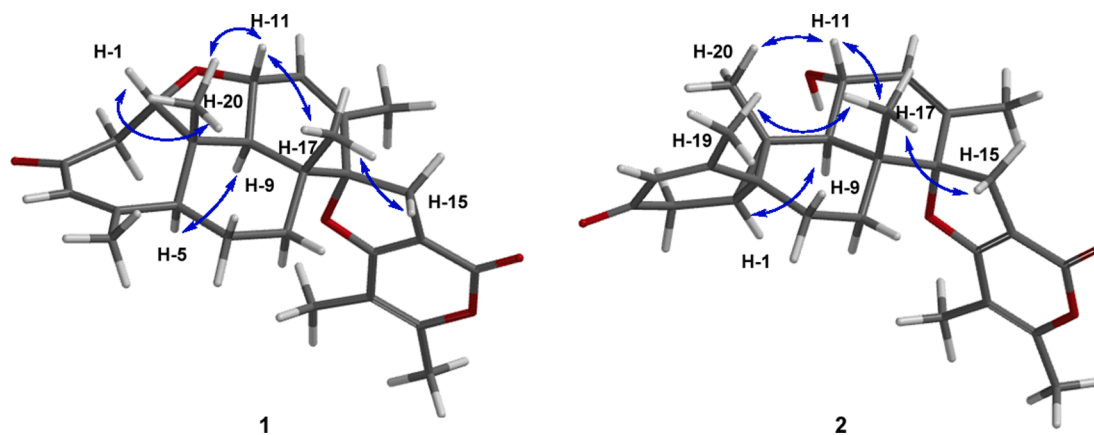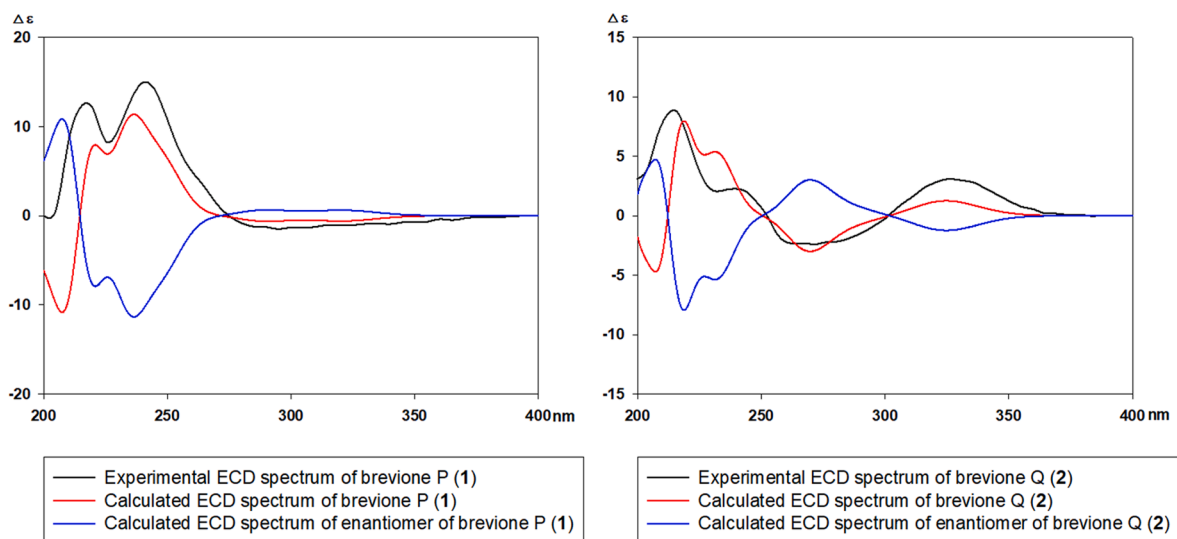
Fig. 3. NOESY NMR correlations of compounds **1** and **2**.

Fig. 4. Experimental and calculated ECD spectra of compounds **1** and **2**.

nm suggested an extended conjugation system. The IR data displayed a strong absorption band at 1718 cm^{-1}, implying the presence of a carbonyl group. The ^{1}H NMR data (Table 1) showed six methyl signals (δ_H 2.22, 1.98, 1.96, 1.74, 1.25, and 1.10), four pairs of geminal methylene signals (δ_H 3.10, 2.98, 2.96, 2.59, 2.10, 1.98, 1.75, and 1.58), two olefinic signals (δ_H 5.95 and 5.83), and two oxygenated methine signals (δ_H 4.27 and 3.77). The ^{13}C NMR data (Table 1) showed 27 resonances comprising six methyl carbons, four methylene carbons, four methine carbons, and 13 non-protonated carbons, including two carbonyl groups. All proton resonances were assigned to the corresponding carbons using heteronuclear single quantum coherence (HSQC) NMR data. Comparing the aforementioned data to those of previously reported breviones suggested that **1** had a partial structure similarity to that of brevione C [9], which has a pentacyclic carbon framework. However, two olefinic signals and geminal methylene signals in brevione C were replaced by newly appeared methylene signals [δ_H 2.96 (H-2a) and 2.59 (H-2b); δ_C 49.3 (C-2)] and two oxygenated methine signals [δ_H 4.27 (H-11) and 3.77 (H-1); δ_C 86.3 (C-1) and 74.4 (C-11)] in **1**. These results indicated the presence of an additional tetrahydrofuran ring produced through oxidative cyclization. Correlation spectroscopy (COSY) and heteronuclear multiple bond correlation (HMBC) NMR data (Fig. 2 and S3–S5) demonstrated the presence of an ether linkage between C-1 and C-11. The relative configuration was determined using nuclear overhauser enhancement spectroscopy (NOESY) NMR data (Fig. 3). NOESY correlations between H-1/H$_3$-20, H-11/H$_3$-20, H-11/H-17, and H-15a/

H-17 indicated that these were oriented on the same side, while those between H-5 and H-9 suggested that the remaining groups had the opposite orientation. The absolute configuration was determined using the ECD calculation method, as described previously [15]. The experimental ECD data showed positive Cotton effects (CEs) at 217 nm ($\Delta\varepsilon$ + 13.3) and 241 nm ($\Delta\varepsilon$ + 15.1), similar to those of previously reported breviones. Furthermore, the experimental ECD data corresponded closely with the calculated data (Fig. 4), suggesting the absolute stereochemistry as 1*S*, 5*S*, 8*R*, 9*R*, 10*S*, 11*R*, and 14*S*. Compound **1** was named brevione P.

Compound **2** was also obtained as a white solid. The molecular formula was the same as that of **1**. The ^{1}H and ^{13}C NMR data of **2** showed that the compound exhibited resonances similar to those of brevione G. However, two methylene signals [δ_H 2.63 (H-2a) and 2.42 (H-2b); δ_C 32.6 (C-2)] and a methine signal [δ_H 1.32 (H-1); δ_C 34.9 (C-1)] were observed in **2** instead of two olefinic signals as found in brevione G [10]. The ^{1}H chemical shift and coupling constant of H-1 (*J* = 9.0 Hz) suggested that C-1 was uniquely connected to two quaternary carbons [δ_C 27.6 (C-5) and 28.2 (C-10)], unlike previously reported breviones. This implied rearrangement of the first seven-membered ring. The HMBC correlations of H-1/C-6 and H-2/C-5 demonstrated the presence of an additional cyclopropane ring because these correlations do not generally appear in the previously reported breviones. Previous studies that described eucarvone tautomerization suggested that a 4-methyl-cyclo-heptadienone ring could be transformed into a 4-methyl-norcarenone
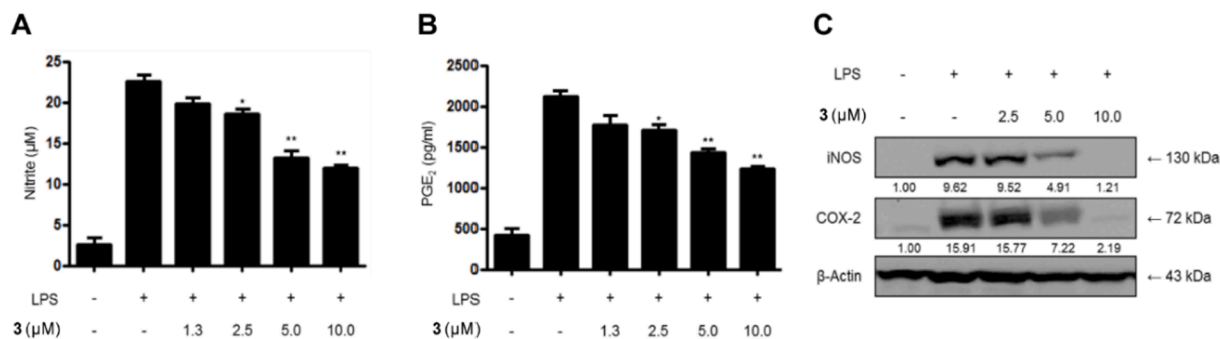
Fig. 5. Effects of compound **3** on NO and PGE$_2$ production and iNOS and COX-2 expression in LPS-stimulated RAW 264.7 cells (A–C). *$p < 0.05$; ***$p < 0.01$ compared to the LPS-treated group.
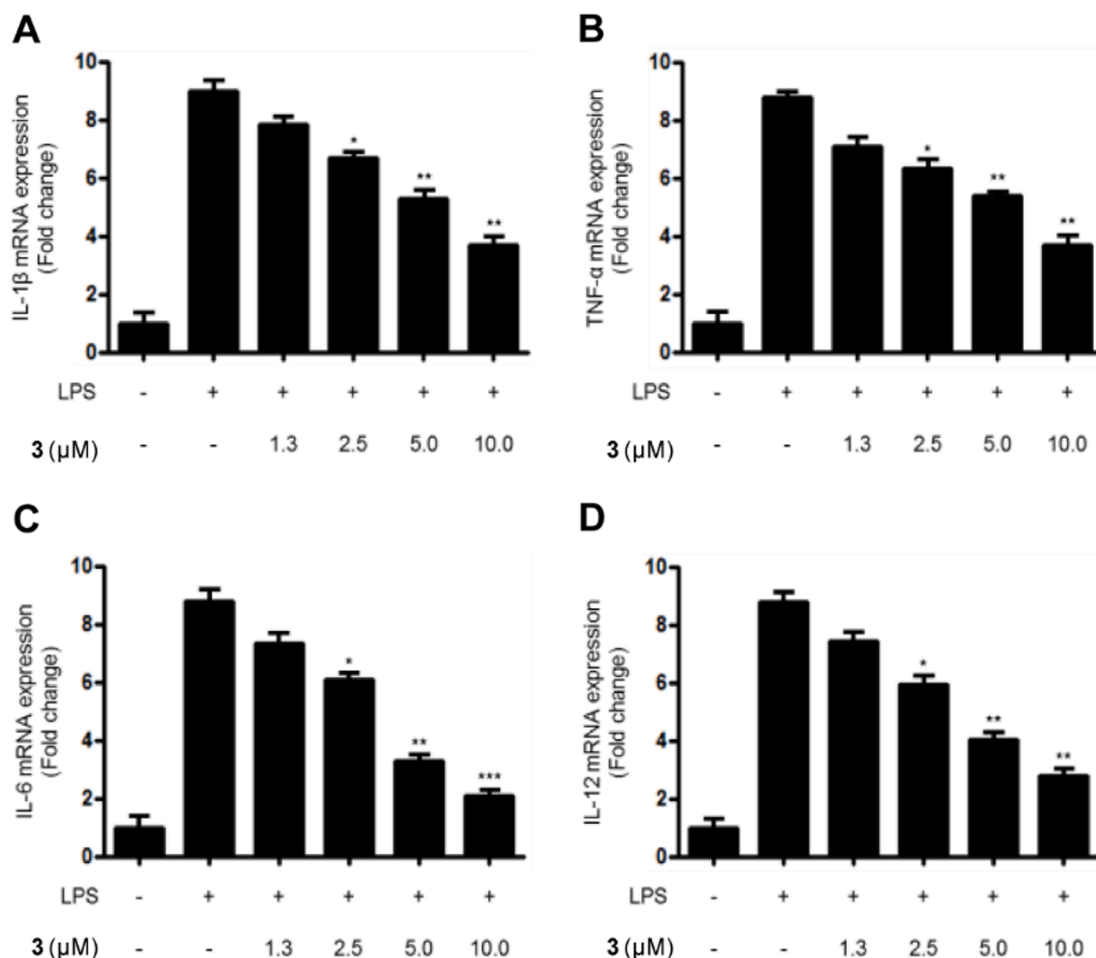

Fig. 6. Effects of compound **3** on IL-1β, TNF-α, IL-6, and IL-12 mRNA expression in LPS-stimulated RAW 264.7 cells. (A–D). *$p < 0.05$; **$p < 0.01$; ***$p < 0.001$ compared to the LPS-treated group.

ring with a bridged bicyclic system [16]. In particular, several diterpenoids, including ebractenoids O and P, which were isolated from *Euphorbia ebracteolata*, are examples of this tautomerization [17]. The whole plane structure was confirmed by a detailed analysis of the 2D NMR data (Fig. 2). The relative configurations at C-1 and C-5 were determined by NOESY correlations between H-1/H-9 and H$_3$-17/H$_3$-19 (Fig. 3). The relative configurations at the remaining positions were the same as those of brevione G [10]. The absolute configuration was determined by the ECD calculation method (Fig. 4). Experimental ECD data showed positive CEs at 214 nm (Δε + 8.8), 239 nm (Δε + 2.3), and 329 nm (Δε + 3.1), which corresponded with the calculated values.

Therefore, the absolute stereochemistry was confirmed as 1*S*, 5*R*, 8*R*, 9*R*, 10*R*, 11*R*, and 14*S*, and compound **2** was named brevione Q.

Additional five compounds were also isolated; these were identified as breviones A (**3**) [9], B (**4**) [9], H [10], and I [11] and deacetylbrevione E [9] by comparing the NMR data with those of known references.

3.2. Anti-inflammatory effects of compounds

All isolated compounds were preliminarily screened using LPS-activated RAW 264.7 cells. Compounds **3** and **4** suppressed NO production (half-maximal inhibitory concentration; IC$_{50}$ = 9.5 ± 0.9 μM for
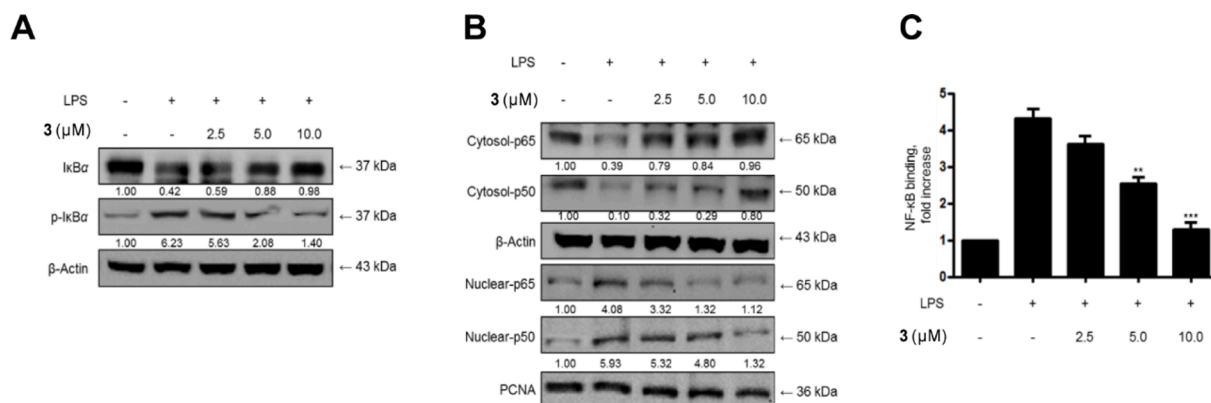
Fig. 7. Effects of compound **3** on the degradation and phosphorylation of IκB, activation of NF-κB, and binding activity of NF-κB in LPS-stimulated RAW 264.7 cells (A–C). **$p < 0.01$ and ***$p < 0.001$ compared to the LPS-treated group.
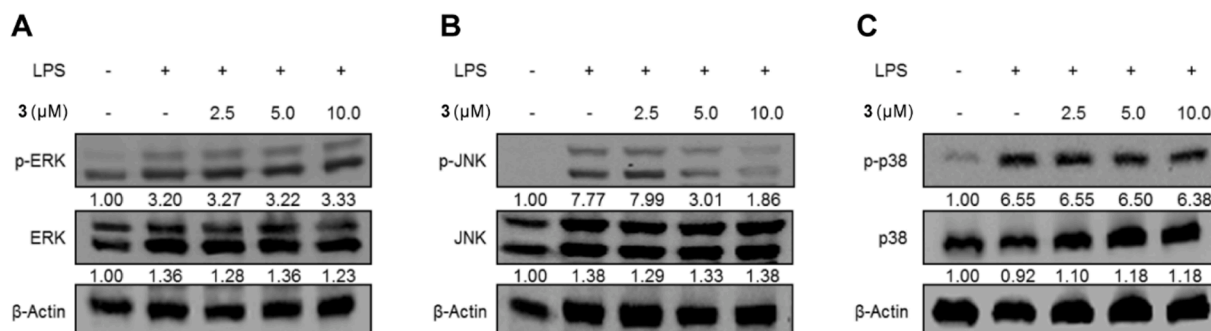

Fig. 8. Effects of compound **3** on ERK, JNK, and p38 MAPK phosphorylation and protein expression.

3 and 21.3 ± 2.0 μM for **4**) without affecting cell viability (Table S1 and Figure S17), while the other compounds were inactive. Compound **3** was selected for further mechanistic studies since this compound showed the most potent activity in the screening assay.

The effects of **3** on NO and PGE_2 production as well as inducible nitric oxide synthase (iNOS) and cyclooxygenase-2 (COX-2) expression were evaluated. Despite LPS stimulation, pretreatment with **3** attenuated not only the expression of inflammatory mediators but also that of iNOS and COX-2 in a dose-dependent manner (Fig. 5). In addition, the effect of **3** on the expression of pro-inflammatory cytokines, such as IL-1β, TNF-α, IL-6, and IL-12, were evaluated. All mRNA levels were downregulated by pretreatment with **3** in a dose-dependent manner (Fig. 6).

The effects of **3** on NF-κB activation and DNA binding were evaluated. Despite LPS stimulation, pretreatment with **3** inhibited phosphorylation and degradation of inhibitor kappa B (IκB) and hindered the nuclear transport of NF-κB subunits (p50-p65). The increased binding activity between NF-κB and DNA caused by LPS stimulation was attenuated by pretreatment with **3** in a dose-dependent manner (Fig. 7).

Finally, the effect of **3** on MAPK phosphorylation was evaluated to identify the role of **3** in MAPK pathway-associated inflammation. Although MAPK phosphorylation increased after LPS stimulation, pretreatment with **3** attenuated c-Jun *N*-terminal kinase (JNK) phosphorylation in a dose-dependent manner, whereas extracellular signal-regulated kinase (ERK) and p38 phosphorylation were not affected (Fig. 8).

4. Conclusions

Breviones have been isolated mainly from *Penicillium* sp., except for breviones L and M, which were isolated from *Aspergillus duricaulis* in our previous study [8,13]. Even though only a limited number of studies

have been conducted, these compounds are of interest not only because of their intriguing structural features but also owing to their biological profiles. The biosynthetic origin of breviones through the mevalonate and acetate pathways has been proposed in a previous report [18]. In a previous study, breviones A–E attenuated etiolated wheat coleoptile growth, and breviones F–H showed cytotoxic activity against HeLa cells [18]. These studies have provided directions for analyzing the synthesis of breviones [19].

In the present study, we isolated seven breviones, including two new compounds (**1** and **2**), from *P. bialowiezense* and investigated the role of these compounds in inflammatory responses. Although some meroterpenoids, including amestolkolides, inhibit NO production [20], to the best of our knowledge, this is the first study to investigate the anti-inflammatory effects of breviones. In the screening procedure, brevione A (**3**) showed an inhibitory effect against NO production with IC_{50} value of 9.5 μM; thus, further mechanistic studies are warranted. In general, pathogenic substances, such as LPS, induce the expression of iNOS and COX with the release of NO and PGE_2 [21]. Inflammatory signals also induce the release of pro-inflammatory cytokines, such as IL-1β, TNF-α, IL-6, and IL-12 [22]. Compound **3** inhibited PGE_2 production and iNOS and COX-2 expression. In addition, compound **3** inhibited the expression of IL-1β, TNF-α, IL-6, and IL-12. Controlling these cytokines is an important therapeutic strategy to overcome several inflammatory diseases. In particular, understanding the signal transduction mechanisms and gene regulation associated with inflammation could provide many opportunities to discover lead compounds for the treatment of various diseases. The NF-κB pathway controls the synthesis of these cytokines by regulating pro-inflammatory gene expression. The NF-κB pathway is activated by the phosphorylation of IκB, thereby releasing p50-p65 heterodimers and allowing them to translocate to the nucleus [23]. MAPKs such as JNK, ERK, and p38 are serine/threonine protein kinases involved in cellular responses to diverse stimuli [24]. Activated MAPKs

also lead to the activation of transcription factors, including NF-κB [25]. Compound **3** inhibited not only the phosphorylation of IκB and nuclear transport of NF-κB subunits but also JNK phosphorylation; in contrast, ERK and p38 levels were not affected. The NF-κB pathway has remained an attractive target for decades because of its critical role in the pathogenesis of inflammatory diseases. However, severe on-target toxicities from NF-κB inhibition have prevented the development of a clinically useful drug [26]. Nonetheless, understanding the signaling networks associated with NF-κB activation could provide critical clues to elucidate the NF-κB conundrum, thus paving the way for safe therapeutics. In the case of the JNK pathway, studies to determine the exact role of JNK are ongoing, and very few JNK inhibitors have entered clinical evaluation [24]. However, recent studies have shown that natural product-derived compounds, such as curcumin and steppogenin, attenuate inflammation by suppressing the NF-κB and JNK signaling pathways [27,28]. Therefore, further studies using breviones should be conducted, which may offer new avenues for the development of breviones as anti-inflammatory drugs.

Declaration of Competing Interest

The authors declare that they have no known competing financial interests or personal relationships that could have appeared to influence the work reported in this paper.

Acknowledgements

Appendix A. . Supplementary material

^{1}H NMR spectral data of known compounds, nucleotide sequence analysis of β-tubulin gene, the screening of all isolated compounds for inhibitory effects of NO production in LPS-activated RAW 264.7 cells, the ^{1}H, ^{13}C, COSY, HSQC, and HMBC NMR, UV, IR, and HRESIMS spectra of compound **1**, the ^{1}H, ^{13}C, COSY, HSQC, and HMBC NMR, UV, IR, and HRESIMS spectra of compound **2**, and the cell viability of compound **3** in RAW 264.7 cells.

Appendix B. Supplementary material

Supplementary data to this article can be found online at https://doi.org/10.1016/j.bioorg.2021.105012.

References

[1] P. Libby, Inflammatory mechanisms: the molecular basis of inflammation and disease, Nutr. Rev. 65 (2007) S140–S146.

[2] S. Harirforoosh, W. Asghar, F. Jamali, Adverse effects of nonsteroidal antiinflammatory drugs: an update of gastrointestinal, cardiovascular and renal complications, J. Pharm. Pharm. Sci. 16 (5) (2013) 821–847.

[3] P. Arulselvan, M.T. Fard, W.S. Tan, S. Gothai, S. Fakurazi, M.E. Norhaizan, S. S. Kumar, Role of antioxidants and natural products in inflammation, Oxid. Med. Cell. Longev. 2016 (2016).

[4] D.H. Yoon, C. Han, Y. Fang, S. Gundeti, I.-S. Han Lee, W.O. Song, K.-C. Hwang, T. W. Kim, G.-H. Sung, H. Park, Inhibitory activity of *Cordyceps bassiana* extract on LPS-induced inflammation in RAW 264.7 cells by suppressing NF-κB activation, Nat. Prod. Sci. 23 (3) (2017) 162–168.

[5] C. Lee, S.H. Shim, Endophytic fungi inhabiting medicinal plants and their bioactive secondary metabolites, Nat. Prod. Sci. 26 (1) (2020) 10–27.

[6] M.J. Kim, D.-C. Kim, J. Kwon, S.M. Ryu, H. Kwon, Y. Guo, S.-B. Hong, Y.-C. Kim, H. Oh, D. Lee, Anti-inflammatory metabolites from *Chaetomium nigricolor*, J. Nat. Prod. 83 (4) (2020) 881–887.

[7] J.-L. Lai, Y.-H. Liu, C. Liu, M.-P. Qi, R.-N. Liu, X.-F. Zhu, Q.-G. Zhou, Y.-Y. Chen, A.-Z. Guo, C.-M. Hu, Indirubin inhibits LPS-induced inflammation via TLR4 abrogation mediated by the NF-κB and MAPK signaling pathways, Inflammation 40 (1) (2017) 1–12.

[8] R. Geris, T.J. Simpson, Meroterpenoids produced by fungi, Nat. Prod. Rep. 26 (8) (2009) 1063–1094.

[9] F.A. Macias, R.M. Varela, A.M. Simonet, H.G. Cutler, S.J. Cutler, F.M. Dugan, R. A. Hill, Novel bioactive breviane spiroditerpenoids from *Penicillium brevicompactum* Dierckx, J. Org. Chem. 65 (26) (2000) 9039–9046.

[10] Y. Li, D. Ye, X. Chen, X. Lu, Z. Shao, H. Zhang, Y. Che, Breviane spiroditerpenoids from an extreme-tolerant *Penicillium* sp. isolated from a deep sea sediment sample, J. Nat. Prod. 72 (5) (2009) 912–916.

[11] Y. Li, D. Ye, Z. Shao, C. Cui, Y. Che, A sterol and spiroditerpenoids from a *Penicillium* sp. isolated from a deep sea sediment sample, Mar. Drugs 10 (2) (2012) 497–508.

[12] B. Yang, W. Sun, J. Wang, S. Lin, X.-N. Li, H. Zhu, Z. Luo, Y. Xue, Z. Hu, Y. Zhang, A new breviane spiroditerpenoid from the marine-derived fungus *Penicillium* sp. TJ403-1, Mar. Drugs 16 (4) (2018) 110.

[13] J. Kwon, Y.H. Seo, J.-E. Lee, E.-K. Seo, S. Li, Y. Guo, S.-B. Hong, S.-Y. Park, D. Lee, Spiroindole alkaloids and spiroditerpenoids from *Aspergillus duricaulis* and their potential neuroprotective effects, J. Nat. Prod. 78 (11) (2015) 2572–2579.

[14] J. Kwon, H. Lee, W. Ko, D.-C. Kim, K.-W. Kim, H.C. Kwon, Y. Guo, J.H. Sohn, J. H. Yim, Y.-C. Kim, H. Oh, D. Lee, Chemical constituents isolated from Antarctic marine-derived *Aspergillus* sp. SF-5976 and their anti-inflammatory effects in LPS-stimulated RAW 264.7 and BV2 cells, Tetrahedron 73 (27–28) (2017) 3905–3912.

[15] J. Kwon, H. Lee, S.M. Ryu, Y. Jang, H.C. Kwon, Y. Guo, J.S. Kang, J.-J. Kim, D. Lee, *Xylodon flaviporus*-derived drimane sesquiterpenoids that inhibit osteoclast differentiation, J. Nat. Prod. 82 (10) (2019) 2835–2841.

[16] L.M. Bateman, O.A. McNamara, N.R. Buckley, P. O'Leary, F. Harrington, N. Kelly, S. O'Keeffe, A. Stack, S. O'Neill, D.G. McCarthy, A.R. Maguire, A study of the norcaradiene–cycloheptatriene equilibrium in a series of azulenones by NMR spectroscopy; the impact of substitution on the position of equilibrium, Org. Biomol. Chem. 13 (45) (2015) 11026–11038.

[17] Z. Yu, Y. Wei, X. Tian, Q. Yan, Q. Yan, X. Huo, C. Wang, C. Sun, B. Zhang, X. Ma, Diterpenoids from the roots of *Euphorbia ebracteolata* and their anti-tuberculosis effects, Bioorg. Chem. 77 (2018) 471–477.

[18] F.A. Macias, C. Carrera, J.C. Galindo, Brevianes revisited, Chem. Rev. 114 (5) (2014) 2717–2732.

[19] H. Yokoe, C. Mitsuhashi, Y. Matsuoka, T. Yoshimura, M. Yoshida, K. Shishido, Enantiocontrolled total syntheses of breviones A, B, and C, J. Am. Chem. Soc. 133 (23) (2011) 8854–8857.

[20] S. Chen, M. Ding, W. Liu, X. Huang, Z. Liu, Y. Lu, H. Liu, Z. She, Anti-inflammatory meroterpenoids from the mangrove endophytic fungus *Talaromyces amestolkiae* YX1, Phytochemistry 146 (2018) 8–15.

[21] T. Tetsuka, D. Daphna-Iken, S.K. Srivastava, L.D. Baier, J. DuMaine, A.R. Morrison, Cross-talk between cyclooxygenase and nitric oxide pathways: prostaglandin E₂ negatively modulates induction of nitric oxide synthase by interleukin 1, Proc. Natl. Acad. Sci. USA 91 (25) (1994) 12168–12172.

[22] C.A. Dinarello, Proinflammatory cytokines, Chest 118 (2) (2000) 503–508.

[23] P.P. Tak, G.S. Firestein, NF-κB: a key role in inflammatory diseases, J. Clin. Invest. 107 (1) (2001) 7–11.

[24] B. Kaminska, MAPK signalling pathways as molecular targets for anti-inflammatory therapy—from molecular mechanisms to therapeutic benefits, Biochim. Biophys. Acta. Proteins. Proteom. 1754 (1–2) (2005) 253–262.

[25] M.B. Alam, M.-K. Ju, Y.-G. Kwon, S.H. Lee, Protopine attenuates inflammation stimulated by carrageenan and LPS via the MAPK/NF-κB pathway, Food Chem. Toxicol. 131 (2019) 110583.

[26] J. Bennett, D. Capece, F. Begalli, D. Verzella, D. D'Andrea, L. Tornatore, G. Franzoso, NF-κB in the crosshairs: Rethinking an old riddle, Int. J. Biochem. Cell Biol. 95 (2018) 108–112.

[27] Y.-R. Chen, T.-H. Tan, Inhibition of the c-Jun N-terminal kinase (JNK) signaling pathway by curcumin, Oncogene 17 (2) (1998) 173–178.

[28] D.-C. Kim, T.H. Quang, H. Oh, Y.-C. Kim, Steppogenin isolated from *Cudrania tricuspidata* shows antineuroinflammatory effects via NF-κB and MAPK pathways in LPS-stimulated BV2 and primary rat microglial cells, Molecules 22 (12) (2017) 2130.